Cerebral Cortex June 2008;18:1415–1420
doi:10.1093/cercor/bhm174
Advance Access publication October 5, 2007

Deep Sulcal Landmarks Provide an Organizing Framework for Human Cortical Folding

Gabriele Lohmann[1], D. Yves von Cramon[1] and Alan C. F. Colchester[2]

[1]Max Planck Institute for Human Cognitive and Brain Sciences, Stephanstr. 1a, 04103 Leipzig, Germany and [2]Kent Institute of Medicine and Health Sciences, Canterbury CT2 7PD, UK

The folding pattern of the cerebral cortex and its relation to functional areas is notoriously variable and there is a need to identify more consistent 3-dimensional (3D) topographical cortical features. We analyzed magnetic resonance brain images of 96 normal adult human volunteers using automated 3D image analysis methods. We examined the deeper parts of the sulci because they generally show less interindividual variability than more superficial parts, especially in monozygotic twins, and deepest parts of primary sulci are the first to develop embryologically and change least as the cortex expands. Along the length of each sulcus we found that there is generally one well-defined zone where depth is maximal, which we term the sulcal pit. Long sulci may have 2 or 3 pits. The spatial arrangement of pits is strikingly regular, forming alternating chains of deeper and shallower pits. We hypothesize that the pits are encoded in the protomap described in Rakic (1988. Specification of cerebral cortical areas. Science. 241:170–176) and are under closer genetic control than the rest of the cortex and are likely to have a more consistent relationship to functional areas.

Keywords: cortical sulci, human cortical folding, magnetic resonance imaging, sulcal pits

Introduction

The high variability of the topography of the cerebral cortex and its relationship to functional areas continues to present challenges for research into cyto- and fiber architecture, neurophysiology, functional activation, and lesion effects as well as for clinical applications (Rademacher et al. 1993). Three specific aspects associated with this variability need to be distinguished. Firstly, even for the most consistent (primary) sulci, which can be identified in all normal individuals and bear a clear relationship to major functional areas, if the boundaries of functional areas can be mapped accurately, as with cytoarchitectonic subdivisions, it becomes clear that they generally do not align accurately with the sulcal fundi (Amunts et al. 2000; Eickhoff et al. 2006). Secondly, for many lesser sulci and gyri that together constitute a large portion of the cortical surface, the geometry is so variable that it may be impossible to establish anatomical correspondence between individuals, reflected in the fact that some folds do not even have well-defined neuroanatomical names (Ono et al. 1990). Thirdly, for the more consistent sulci and gyri that can be compared between individuals, their locations, typically expressed in coordinates based on the anterior and posterior commissures (AC and PC), show high interindividual variation (eg, a range of ±10 mm for central and calcarine sulci) (Talairach and Tournoux 1988; Ono et al. 1990; Steinmetz et al. 1990).

From a functional point of view, the cortex can be viewed as a 2D processing manifold and this has led to the development of approaches to improve visualization of the manifold and of surface-based coordinate systems to express the spatial relationship of functional or anatomical features on the manifold (van Essen 2005). The variable relation of many 3-dimensional (3D) topographical features (gyri and sulci) to functional areas is well shown on such maps, although the precision of the different methods involved places clear limits on detailed interpretation (van Essen et al. 1998).

It would greatly assist the mapping of function to structure if 3D topographical cortical features could be identified, which were more consistent between individuals than the majority of the folding pattern and which bore a more consistent relationship to functional areas. For 2 reasons, we hypothesized that the deepest parts of the sulcal fundi would be the most likely to satisfy these requirements. Firstly, quantitative studies of intersubject variation revealed that the sulcal pattern becomes more consistent at increasing depths below the surface (Le Goualher et al. 1999; Lohmann et al. 1999), particularly in monozygotic twins (Lohmann et al. 1999), indicating increasing genetic influence with depth. Secondly, the deepest parts of sulci form early and retain their identity during development; the more complex (and variable) superficial folds form later (Smart and McSherry 1986; Welker 1990). There is abundant evidence that the basic functional organization of the cortical manifold is laid down in the fetal ventricular zone (the "protomap" of Rakic [Rakic 1988, 2004; Piao et al. 2004]), where cortical neurones are formed from progenitor cells before they migrate superficially along a radial glial scaffolding to form the cortical surface. Therefore, it is likely that the deepest parts of the sulci have a specific spatial relationship to functional areas as well as having ontogenetic importance.

In the present study, we developed a method for extracting the deepest parts of the sulcal fundi, which we term the sulcal "pits," and examined their spatial distribution in a large group of individuals.

Materials and Methods

Data Acquisition and Initial Processing

Our data pool consisted of 48 female and 48 male right-handed normal human subjects aged between 18 and 60 years (mean 29.2). The data were acquired in the context of various functional magnetic resonance imaging (MRI) experiments conducted at the Max Planck Institute for Human Cognitive and Brain Sciences, Leipzig, Germany, between January 2001 and August 2002. All subjects gave informed consent. All subjects received a high-resolution *T1*-weighted MRI scan acquired on a 3-T magnetic resonance scanner (Bruker Medspec 300, Ettlingen,

Germany) using a modified driven equilibrium Fourier transform pulse sequence. Resolution was set to 1 × 1 mm within plane and 1.5 mm between planes. All datasets were initially coregistered using a standard approach based on the AC and PC (Talairach and Tournoux 1988). For this, the upper rim of AC in the median sagittal plane was taken as the origin and trilinear scaling (derived separately in antero–posterior, lateral, and supero–inferior directions from the bounding box on the outer cerebral surface) was applied to each dataset. At the same time, the datasets were resampled to produce isotropic 1 × 1 × 1 mm voxels. In addition to the affine linear registration to the AC/PC-based coordinate system, we performed a nonlinear registration to the generic gyral model (GGM) as introduced in (Lohmann et al. 2005, 2006). The GGM contains a polygonal line–based representation of 6 major cortical gyri obtained as a population average. The registration caused those 6 major gyri to be geometrically aligned in all 96 datasets. The images were then segmented to extract the cerebral white matter, removing nonbrain structures and cortical gray matter, to make sulcal indentations easier to describe and analyze. All subsequent image analysis procedures were based on these coregistered datasets in which the white matter was segmented. The automated segmentation procedures are less reliable for orbital, basal, medial, and insular cortices, and we have restricted the current study to the lateral cortex.

Data Analysis

Our experimental results are based upon automatic image analysis methods applied to the preprocessed MRI data. We extracted a smooth superficial white matter surface with a morphological closing operation using a spherical structuring element of radius 15 mm and referred to this as the "closed" surface. This would correspond to the arachnoid surface if the gray matter were included. Similarly, we extracted a deep white matter surface resembling a primitive unfolded or lissencephalic brain with a morphological opening operation using a spherical structuring element of radius 5 mm and referred to this as the "opened" surface. A distance transform was then computed inside the closed surface, giving the absolute depth of any point measured from this surface (Fig. 1). We automatically segmented all major sulci in an individual and extracted their depth profiles along their entire length (see Fig. 2). We also calculated the depth of points in sulci as a percentage of the distance between the closed (superficial) and opened (deep) white matter surfaces at any point and referred to this as the "relative depth" (Fig. 1).

Segmentation of Sulcal Pits

To investigate the spatial distribution of the deepest parts of the sulci across individuals, while eliminating minor local variations in the depth profile, we carried out the following steps. We first located all local relative depth maxima on the white matter surface, defined by there being no deeper voxel within a diameter of 5 mm. Starting from each local maximum, we created a small region by linking all voxels that shared a common face (26-connected) with the starting point and that were no more than 5% relative depth shallower than the local maximum. This procedure had the effect of "flooding" the neighborhood of each local maximum, filling a small local region, which we refer to as the "sulcal pit."

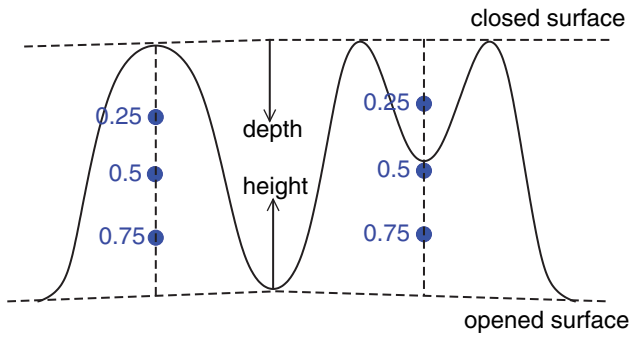

Figure 1. Definition of relative depth. Relative depth measures the relative distance from the deep white matter surface to the superficial white matter surface. The deep white matter surface is approximated by a morphological opening filter that removes major gyri. Major sulci are deep and minor sulci are shallow by this definition of depth.

Results

We analyzed several properties of sulci as a function of depth as measured from the outer brain surface. When the sulci fundi were examined along their full length, and local fluctuations over a scale of a few millimeters are removed, most sulci had only one depth minimum or pit (Fig. 2). However, for certain major sulci, there may be more than one: the central sulcus usually has 2 and the superior frontal sulcus usually has 3 or 4. Note that a sulcal pit is a locally deepest part of a sulcal base or fundus, the fundus extending along the full length of the sulcus. The longer sulci, mostly corresponding to the traditional primary sulci, extend down to the closed (deep) white matter surface, and we refer to any such sulcus as "major" and to shallower pits as "minor." We have avoided the terms "primary" and "secondary," which are not used consistently in the literature.

The sulci have fewer branches at deeper levels than they do superficially. Their pattern becomes notably more consistent across subjects, and it is much easier to identify interindividual homologies of sulcal pits rather than homologies of entire sulci. Figure 3 shows the sulcal pattern of 2 individuals at 4 different levels of depth. The superficial sulcal pattern in the region of the angular gyrus in the left hemisphere differs markedly in the 2 individuals, but at increasing levels of depth (rows 2 and 3), it becomes clear that the sulcal pattern becomes simpler and progressively more similar and at depth levels between about 50% and 60% reduces to a pit in a similar location. The pit has disappeared by the 86% depth level (bottom row of Fig. 3), and we therefore classify the pit as minor.

Using the center of gravity of a pit as a point marker for sulcus locations, we analyzed the variation of pits across all 96 subjects. Figure 4 shows that the pit locations form significant clusters not only for major but also for minor sulci. This regularity of minor and major sulci only became apparent when we investigated their deepest regions represented as points in 3D space.

Table 1 gives the loci of centers of major pit clusters and their densities and the anatomical names of the sulci to which they usually correspond. Similarly, Table 2 gives the loci and densities of minor pit clusters. Note that pits in some clusters may belong to sulci with different names in different individuals because of the variation of superficial folding patterns (Fig. 3), and for minor clusters, we have omitted possible sulcus names. Supplementary Figures 1–4 and their accompanying videos provide further views of the original data.

The clusters form chains stretching from the anterior pole toward the posterior pole and from the temporal pole toward the intraparietal lobe, shown diagrammatically in Figure 5. A prominent chain of clusters of minor sulcal pits is located along the frontal and parietal opercula extending further posterior into the posterior parietal and parietal–occipital cortex (clusters b, c, d, and e of Fig. 5 and Table 1). The general arrangement of the chains of pits seems to follow the alignment

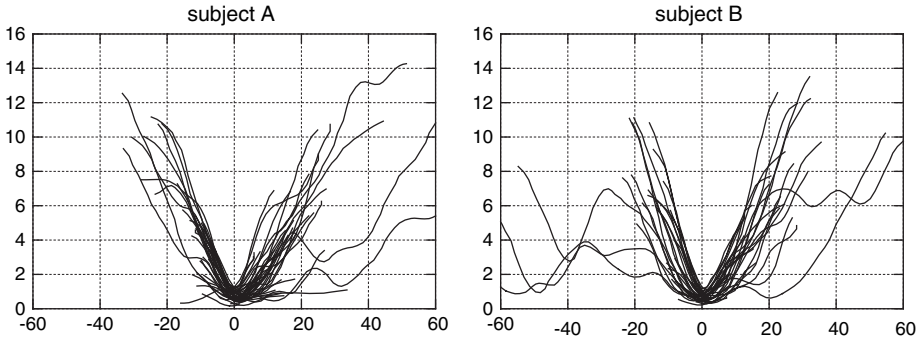

Figure 2. Depth profiles of sulcal fundi in 2 subjects. All major sulci were automatically segmented. The absolute depths of the fundi along their entire length are plotted as a function of the distance along the sulcal fundus from the deepest point. The *x* axis shows the distance along the fundus in millimeters. The *y* axis shows the depth in millimeters, normalized at each point by subtracting the depth of the deepest point. The data are smoothed using a Gaussian kernel with $\sigma = 2$. Note that most of the profiles have a focused central region. The sulcal pits are in the center of these deepest regions.

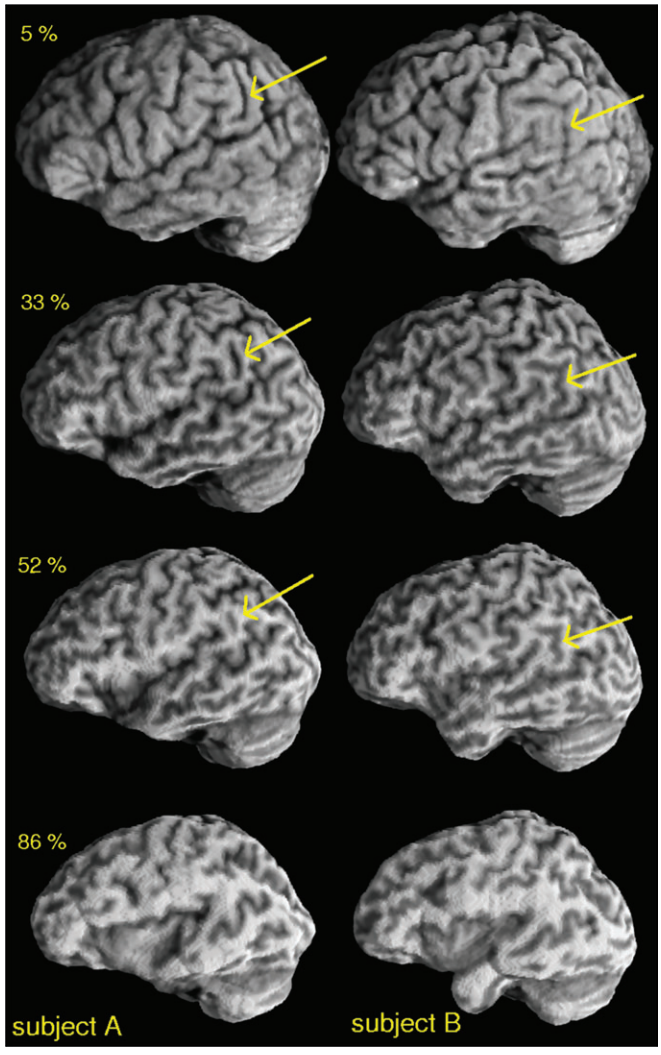

Figure 3. Complexity of sulcal pattern decreases with depth. This image shows the sulcal patterns of 2 individuals at 4 different levels of depth. Note in particular a sulcus within the angular gyrus marked by an arrow. Using Ono's classification, the marked sulcus in the right image (subject A) would be called "primary intermediate sulcus" as it is a side branch of the intraparietal sulcus, whereas the marked sulcus in the left image (subject B) is the "angular sulcus" as it is a branch of the superior temporal sulcus. However, at the innermost depth level, it becomes clear that the 2 sulci have a common pit suggesting that they are morphologically homologous. The pit belongs to the cluster labeled "d" in Table 2 and Figure 5.

of the underlying lateral ventricles (Fig. 6). Minor chains are interleaved with major chains. Further clusters can be found within the middle temporal gyrus and the lateral occipital gyri and at the occipital polar cap.

Discussion

We have shown that when the extended space curves constituting sulcal fundi are reduced to the locally deepest points or sulcal pits, the spatial relationship between sulci becomes much clearer and forms striking alternating major and minor chains of pits. The chains correspond well with the distribution of areas of highest heritability of gray matter density described by Thompson (Thompson et al. 2001).

We hypothesize that the pits are encoded in the protomap of prospective cytoarchitectonic areas (Rakic 1988) and are under closer genetic control than the rest of the cortex. This leads to predictions that should be tested in future research. Because the broad arrangement of functional areas is also encoded in the protomap, we predict that the spatial correlation between sulcal pits and functional areas should be much clearer than with other sulcal features. This could be examined in several ways. We would expect that the pits have a more consistent relationship to cytoarchitectonic areas than is generally the case for sulcal fundi (Amunts et al. 2000)—even though the relationship between sulcal features and cytoarchitectonic areas may be nonlinearly distorted during the process of gyrogenesis and therefore difficult to identify in adult brains. The location of pits in relation to data from functional activation, neurophysiology, and fiber architecture studies should also be examined.

Although this evidence indicates the importance of genetic factors in explaining relative consistency of pit locations across individuals, the ontogenetic determinants of the more variable, later-developing superficial cortical folds need further consideration. There is a growing body of evidence that axonal tension forces are important in the formation of cortical folds (gyrogenesis) (Scannell 1997; van Essen 1997; Hilgetag and Barbas 2006). The timing of development of cortical connections is consistent with a causal role, and disruption of connections during development has a marked effect on the gyral pattern (Goldman-Rakic 1980). Thus, it seems likely that the density of axonal connections is important in determining the location of many sulci and gyri, and variation in axonal

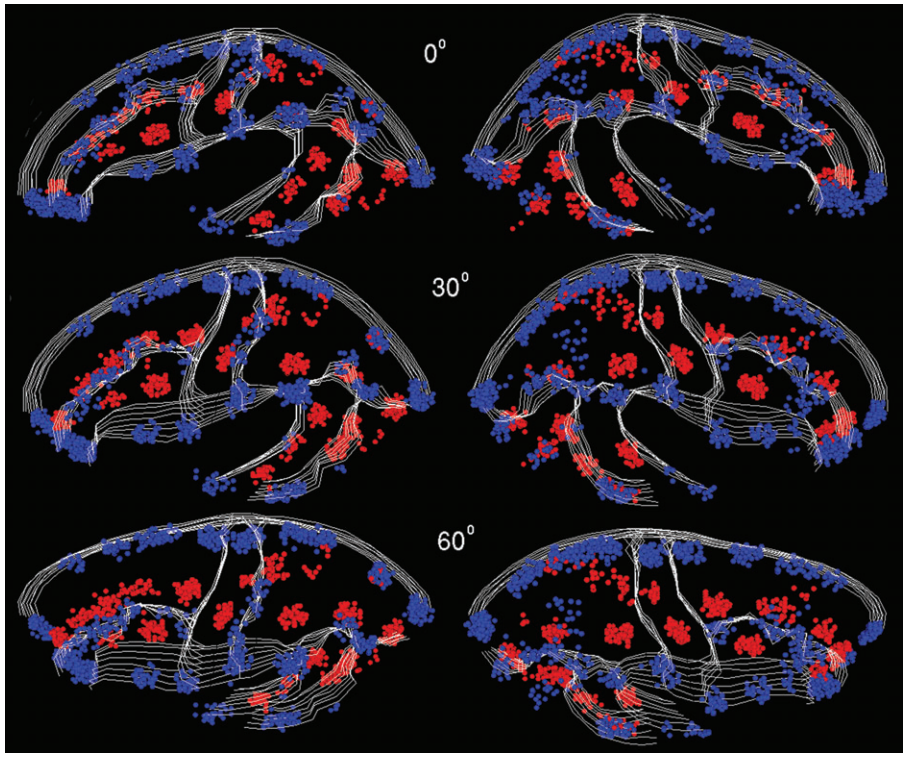

Figure 4. Location of major and minor sulcal pits from the group of 96 subjects. Left and right lateral views are shown in the left and right columns; rows show degrees of rotation from true lateral (top row) toward a more superior viewpoint. Pits of major sulci are shown as red spheres, minor as blue. The pit clusters are arranged in interleaved chains that mark a clear spatial separation between these 2 types of pits. For clarity, only regions where pit density was maximal are shown. The GGM that served as a template for nonlinear registration is shown as white lines. See also Supplementary Video 1 and Supplementary Figure 1.

Table 1
Major sulcal pits

Pit label	Left hemisphere				Right hemisphere				Sulcus name
	Address			Density	Address			Density	
A	−31	33	13	39	29	28	22	23	Inferior frontal sulcus
B	−32	6	29	66	30	7	29	73	Junction of inferior precentral and inferior frontal sulcus
C	−33	−16	40	86	31	−17	39	85	Central sulcus, inferior part
D	−30	−40	37	54	30	-33	38	64	Intraparietal sulcus, horizontal branch
E	−26	−60	31	57	27	−60	31	58	Intraparietal sulcus, descending branch
F	−24	23	34	32	23	31	29	38	Superior frontal sulcus, anterior part
G	−26	−6	45	74	24	−4	45	65	Junction of superior precentral and superior frontal sulcus
H	−24	−25	51	38	24	−24	51	30	Central sulcus, superior part
I	−45	−31	2	46	40	−33	6	68	Superior temporal sulcus, middle part
J	−37	−51	22	51	37	−46	23	31	Superior temporal sulcus, posterior part
K	−35	−63	15	57	36	−55	15	75	Transverse occipital sulcus

Note: The labels for the pits correspond to those in Figure 5. The addresses give the AC–PC coordinates of the center of the sulcal pit clusters (local maxima in the distribution map). The density is the percentage of subjects having a pit within a radius of 5 mm around each cluster center. The sulcus name follows as far as possible the conventions established by Ono (Ono et al. 1990).

density could explain the variations in the pattern of superficial sulci.

If pits are confirmed as having a clearer relation to functional areas than other geometrically defined features, important applications will follow. In particular, the sulcal pits can be used as landmarks to refine the current methods for interindividual and atlas-to-individual coregistration, both for traditional 3D methods that are based on deep landmarks and the outer (arachnoid) brain surface, and in the newer surface-based approaches (van Essen 2005).

Notes

Conflict of Interest: None declared.

Address correspondence to Gabriele Lohmann, Max Planck Institute for Human Cognitive and Brain Sciences, Stephanstr. 1a, 04103 Leipzig, Germany. Email: lohmann@cbs.mpg.de.

Table 2
Minor sulcal pits

Pit label	Left hemisphere				Right hemisphere			
	Address			Density	Address			Density
a	−43	11	16	40	42	12	17	31
b	−50	−4	20	46	48	−2	19	35
c	−46	−23	31	51	40	−21	36	41
d	−49	−42	35	57	48	−35	38	43
e	−38	−67	30	48	38	−55	35	30
f	−15	−91	11	85	15	−88	14	81
g	−32	−76	11	25	Not present			
h	−52	−41	−4	38	47	−40	−3	61
i	−49	−14	−3	21	50	−8	−2	13
j	−29	−30	55	18	Not present			
k	−33	25	32	25	32	24	37	19
l	−35	34	2	86	32	40	5	59

Note: For explanation, see Table 1 and Figure 5. For minor sulci, naming is very inconsistent and anatomical names are omitted.

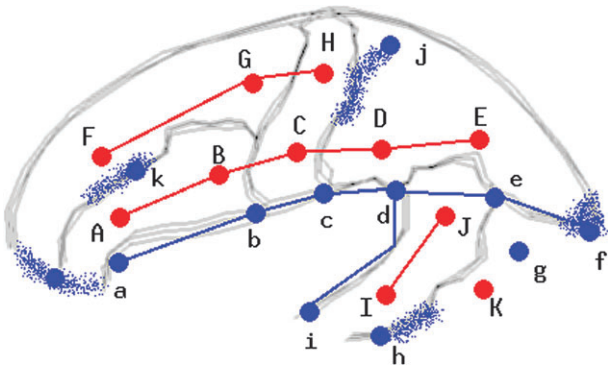

Figure 5. Chains of sulcal pits. The most prominent chains are in an antero–posterior orientation. Pit labels correspond to those in Table 1: major sulcus pits are labeled in capitals, minor in lower case. Some clusters of minor pits are not well localized (j, k, h, f, and l) and are therefore shown as fuzzy clouds.

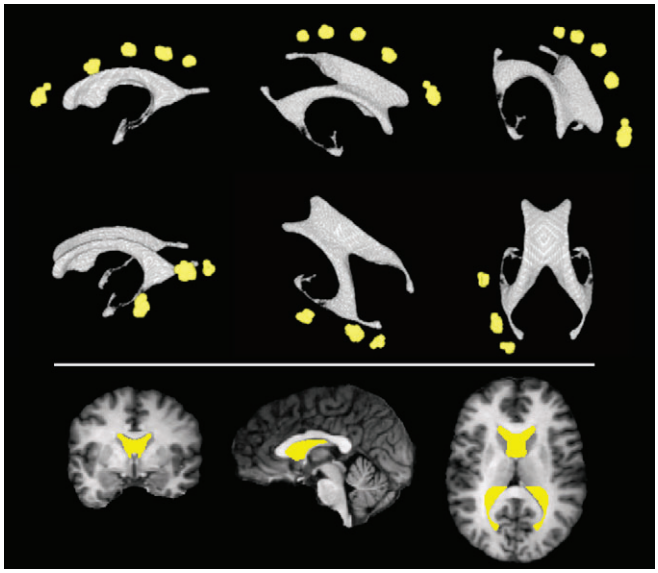

Figure 6. Relations between pit chains and the lateral ventricles. The upper panel shows the spatial relation of the sulcal pits to the lateral ventricles. For better visualization, only 2 chains of major pits of the left hemisphere are shown. The other chains are roughly parallel. Note that both chains are approximately equidistant to the ventricular surface. The ventricle mask represents an average shape that was generated semiautomatically using *T1*-weighted MRI data of several subjects. The lower panel shows the mask superimposed on an MRI image of 1 subject.

References

Amunts K, Malikovic A, Mohlberg H, Schormann T, Zilles K. 2000. Brodmann's areas 17 and 18 brought into stereotaxic space—where and how variable? NeuroImage. 11:66–84.

Eickhoff SB, Hein S, Zilles K, Amunts K. 2006. Testing anatomically specified hypotheses in functional imaging using cytoarchitectonic maps. NeuroImage. 32:570–582.

Goldman-Rakic PS. 1980. Morphological consequences of prenatal injury to the primate brain. Prog Brain Res. 53:1–19.

Hilgetag CC, Barbas H. 2006. Role of mechanical factors in the morphology of the primate cerebral cortex. PLos Comput Biol. 2(3):e22.

Le Goualher G, Procyk E, Collins DL, Venugopal R, Barillot C, Evans AC. 1999. Automated extraction and variability analysis of sulcal neuroanatomy. IEEE Transactions on Medical Imaging. 18: 206–217.

Lohmann G, von Cramon DY, Colchester ACF. 2005. Construction of an averaged representation of human cortical gyri using non-linear principal component analysis. In: Duncan J, Gerig G, editors. Medical image computing and computer-assisted intervention. Vol. 2. Berlin (Germany): Springer. p. 749–756.

Lohmann G, von Cramon DY, Colchester ACF. 2006. Investigating cortical variability using a generic gyral model. In: Larsen H, Nielsen M, Sporring N, editors. Medical image computing and computer-assisted intervention. Vol. 2. Berlin (Germany): Springer. p. 109–116.

Lohmann G, von Cramon DY, Steinmetz H. 1999. Sulcal variability of twins. Cereb Cortex. 9:754–763.

Ono M, Kubik S, Abernathey CD. 1990. Atlas of the cerebral sulci. Stuttgart: Thieme.

Piao X, Hill RS, Bodell A, Chang BS, Basel-Vanagaite L, Straussberg R, Dobyns WB, Qasrawi B, Winter RM, Innes AM, et al. 2004. G protein-coupled receptor-dependent development of human frontal cortex. Science. 303:2033–2036.

Rademacher J, Caviness VS, Steinmetz H, Galaburda AM. 1993. Topographical variation of the human primary cortices: implications for neuroimaging, brain mapping, and neurobiology. Cereb Cortex. 3:313–329.

Rakic P. 1988. Specification of cerebral cortical areas. Science. 241:170–176.

Rakic P. 2004. Genetic control of cortical convolutions. Science. 303:1983–1984.

Scannell JW. 1997. Determining cortical landscapes. Nature. 386:452.

Smart IHM, McSherry GM. 1986. Gyrus formation in the cerebral cortex in the ferret. I. Description of the external changes. J Anat. 146:141–152.

Steinmetz H, Furst G, Freund H-J. 1990. Variation of perisylvian and calcarine anatomic landmarks within stereotaxic proportional coordinates. Am J Neuroradiol. 11:1123–1130.

Talairach J, Tournoux P. 1988. Co-planar stereotaxic atlas of the human brain. New York: Thieme.
Thompson PM, Cannon TD, Toga AW. 2001. Genetic influences on human brain structure. Nat Neurosci. 4:1253–1258.
van Essen DC. 1997. A tension-based theory of morphogenesis and compact wiring in the central nervous system. Nature. 385:313–318.
van Essen DC. 2005. A population-average, landmark- and surface-based (PALS) atlas of the human cerebral cortex. NeuroImage. 28:635.
van Essen DC, Drury HA, Joshi S, Miller MI. 1998. Functional and structural mapping of human cerebral cortex: solutions are in the surfaces. Proc Natl Acad Sci USA. 95:788–795.
Welker W. 1990. Why does cerebral cortex fissure and fold? A review of determinants of gyri and sulci. In: Jones EG, Peters A, editors. Cerebral cortex: comparative structure and evolution of cerebral cortex. Part II. Vol. 8B. New York: Plenum Press. p. 3–136.